

University of New Hampshire

University of New Hampshire Scholars' Repository

Honors Theses and Capstones

Student Scholarship

Spring 2022

Investigating Signs of Orbital Decay in the TrES-1 Exoplanetary System

Amanda F. Wester

University of New Hampshire, Durham

Follow this and additional works at: <https://scholars.unh.edu/honors>



Part of the [Other Astrophysics and Astronomy Commons](#), [Physical Processes Commons](#), and the [The Sun and the Solar System Commons](#)

Recommended Citation

Wester, Amanda F., "Investigating Signs of Orbital Decay in the TrES-1 Exoplanetary System" (2022).

Honors Theses and Capstones. 782.

<https://scholars.unh.edu/honors/782>

This Senior Honors Thesis is brought to you for free and open access by the Student Scholarship at University of New Hampshire Scholars' Repository. It has been accepted for inclusion in Honors Theses and Capstones by an authorized administrator of University of New Hampshire Scholars' Repository. For more information, please contact Scholarly.Communication@unh.edu.

Investigating Signs of Orbital Decay in the TrES-1 Exoplanetary System

Amanda F. Wester

May 24, 2022

Abstract

Transit observations of exoplanetary systems can be used to investigate orbital decay. TrES-1b is an exoplanet hypothesized to be experiencing orbital decay due to observed transit timing variations (TTVs) [12]. Numerous transits must be observed to establish a long term pattern to conclusively determine if the planet's orbit is decaying. Measurements were made using the UNH Observatory where 2 transits were observed of the TrES-1b transiting system on February 27, 2022 and March 5, 2022. A CCD camera was used to image the transit and capture calibration images. The software AstroImageJ (AIJ) was used to calibrate the images and perform photometry to generate a light curve (LC) for the target star through the duration of the transit observation. The center of the transit can be calculated from the light curve given that AIJ is able to fit a light curve trendline to the LC. The data from the observed transits yielded inconclusive results as AIJ was unable to fit a light curve to the data and thus unable to find the transit center. The largest sources of error were cloud cover in the region of observation and improper telescope tracking. Understanding these sources of error allows for their effects to be mitigated in future data collection

1 BACKGROUND

1.1 Exoplanets

Exoplanets are planets that orbit a star other than our own. The first confirmed exoplanets were found orbiting the pulsar PSR1257+12 by Aleksander Wolszczan and Dale Frail in 1992 [13]. These exoplanets were discovered using the radial velocity method, which consists of measuring the “wobble” of a star by looking for evidence of red or blue-shifting in the star’s spectrum over time. As of May 2022, there are over 5000 confirmed exoplanets [3]. A large portion of these were discovered by NASA’s Kepler mission that used the transit method, which involves observing a star’s decrease in apparent brightness when a planet passes in front of it as viewed from Earth.

As exoplanet research progresses, more is being learned about the structure of solar systems and the underlying physics behind their formation and evolution. Nearly 85% of discovered exoplanets are in the tidal-locking zone [7], where tidal-locking refers to the same side of the planet always facing the star. These are the easiest to detect because close-in planets exert the largest effects on their host stars. Generally, their effects can also be observed over relatively short time periods on the order of several days to less than an hour [3]. Studying these exoplanets is an effective way to learn about planetary system formation and dynamics because a variety of systems with diverse characteristics can be observed.

1.2 Orbital Decay

Orbital decay in a planet-star system refers to a decrease in separation between the star and planet over time. Specifically, it is the decrease in the planet’s perigee, the closest point in the planet’s orbit. Orbital decay occurs due to a friction-driven process where energy is transferred or dissipated from the orbit of the planet into a different part of the solar system. One such mechanism is tidal dissipation where energy from the planet’s orbital angular momentum is dissipated into the star.

Tidal theory postulates that while two rigid bodies can maintain a stable orbit forever, stars and planets are not rigid bodies and can be deformed, possibly resulting in an unstable orbit. Stars behave like fluids, thus they can produce tides due to gravitational attraction, similar to how there

are tides in Earth's oceans due to the Moon and Sun's gravity. Stars can have high and low tides in different regions and they become ellipsoids. Planets in tidally locked orbits around their host star can also be deformed into ellipsoids. As the planet pulls gravitationally on the star, some of the star's orbital angular momentum is transferred into spin angular momentum and the star will rotate faster. The planet's orbital angular momentum will decrease with the star's as energy from the orbit is dissipated through tidal heating of the planet [10].

Various processes can also cause the appearance of orbital decay where there may be none, such as apsidal precession or the presence of another planet. Apsidal precession occurs as the orbital path of the planet slowly rotates around the star with each successive orbit. These effects create the necessity to observe an apparently decaying system over a sufficiently long period of time to rule out the illusion of orbital decay caused by other processes.

1.3 Transit Timing Variations

Transit timing variations (TTVs) are changes in the time spacing between successive transits. Transit duration variations (TDVs) are also investigated when searching for evidence of an additional planet or an exomoon (a natural satellite around an exoplanet), however TTVs are considered more heavily when investigating orbital decay in a system [9]. As the orbit of a planet decays, there will be a measurable change in the time between successive transits. Figure 1 is an O-C plot of the decaying exoplanet Wasp-12b that depicts the calculated mid-transit time subtracted from the observed mid-transit time for a data set. The difference between the observed and calculated transit centers is due to TTVs. The large deviations from 0.00 on the vertical axis are indicative of orbital decay. Figure 2 is an O-C plot for TrES-1b where the plot visually looks flat because more data is needed over a long period of time.

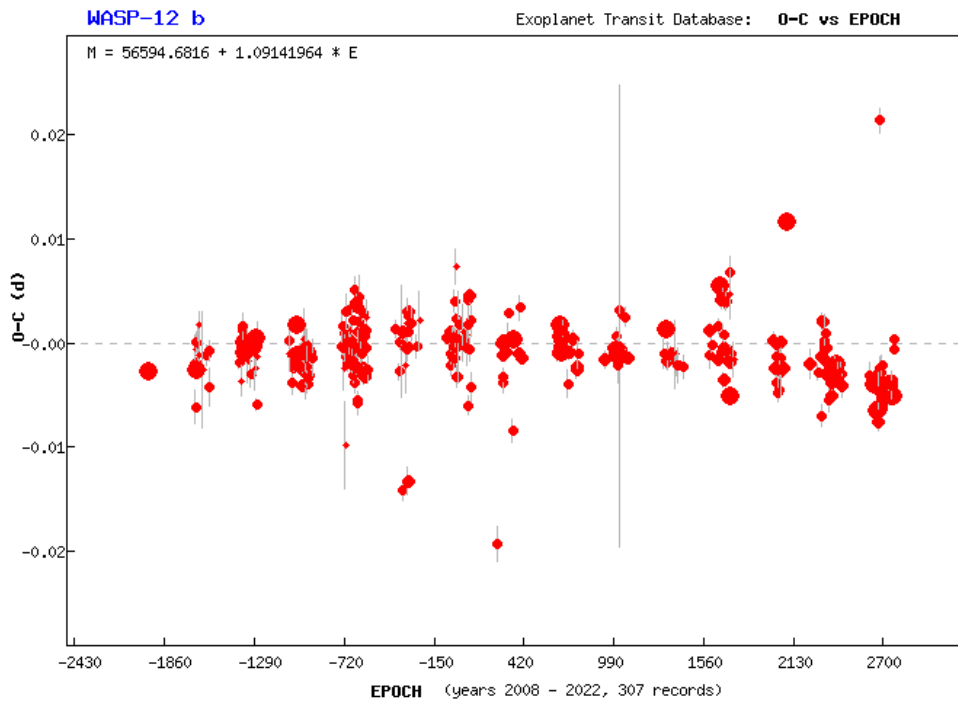


Figure 1: An O-C plot of the decaying exoplanet Wasp-12b from the Exoplanet Transit Database ([Wasp-12b](#)) [4]. Larger dots depict more reliable data.

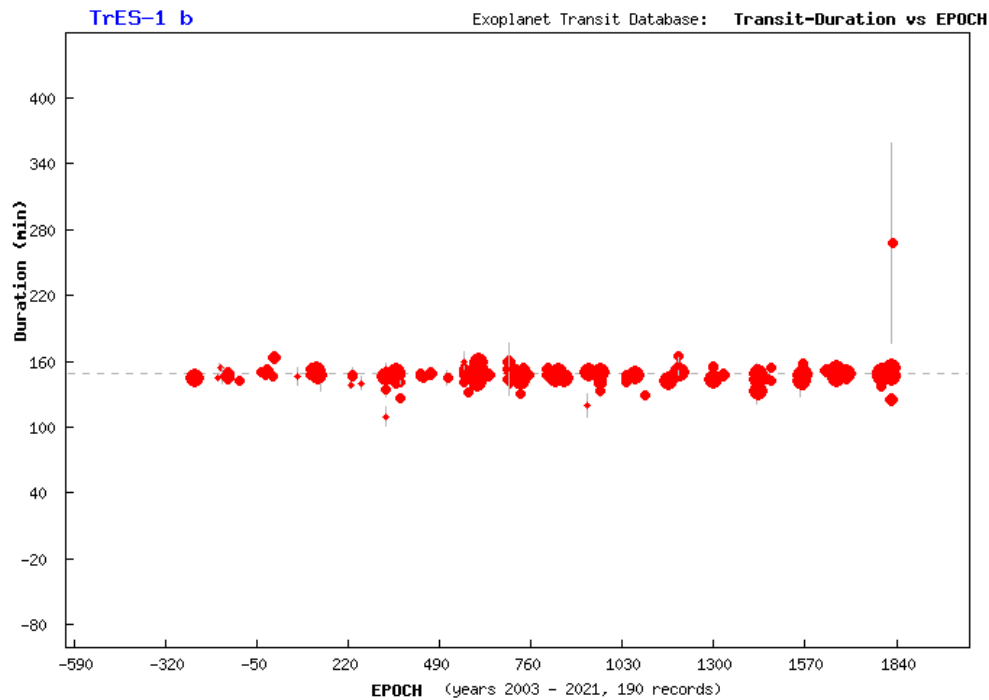


Figure 2: An O-C plot for TrES-1b from the Exoplanet Transit Database ([TrES-1b](#)) [4]. Larger dots represent more reliable data.

1.4 TrES-1b

Discovered in 2004, TrES-1b was the first exoplanet discovered as part of the Trans-atlantic Exoplanet Survey (TrES) [6]. The coverage area is located in the constellation Lyra and figure 3 shows the starfield for the TrES-1 system. The planet TrES-1b is a Jupiter-like gas giant whose mass is $0.761 M_J$ and whose radius is $1.099 R_J$ [11]. TrES-1b is an ideal target for orbital decay research because it has a frequent orbital period of 3.03 days [3] and a transit depth, or decrease in brightness during the transit, of ~2% [4].

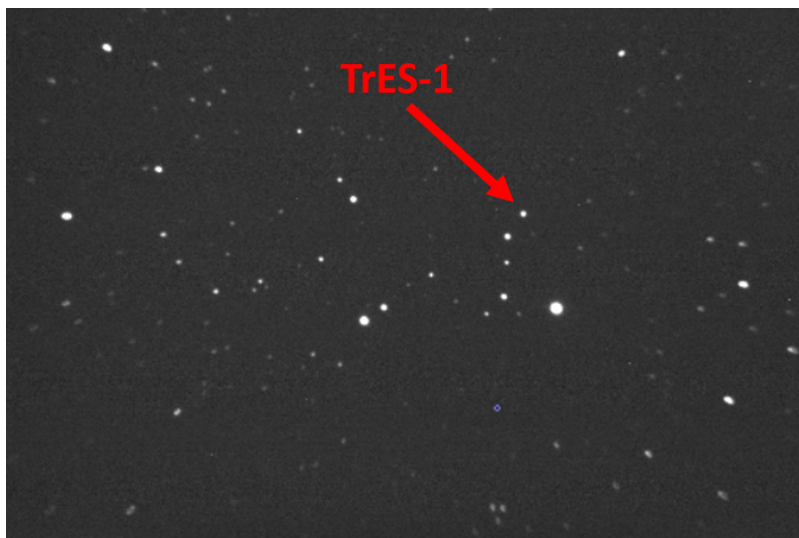


Figure 3: The star field of TrES-1 with the location of the system indicated.

2 DATA COLLECTION

2.1 Exoplanet Detection Methods

2.1.1 Transit Method

The transit method utilizes a star's decrease in apparent brightness when a planet passes in front of it in an observer's line of sight. When a planet transits, its brightness decreases during its passage across its host star. Once the planet moves off the star, the star's

brightness returns to its previous level. The size of the planet will dictate how much the star's brightness decreases. The star's brightness during the transit can be shown on a plot called a light curve (LC). The transit begins at the ingress and ends at the egress. Figure 4 shows what happens during different stages of a transit.

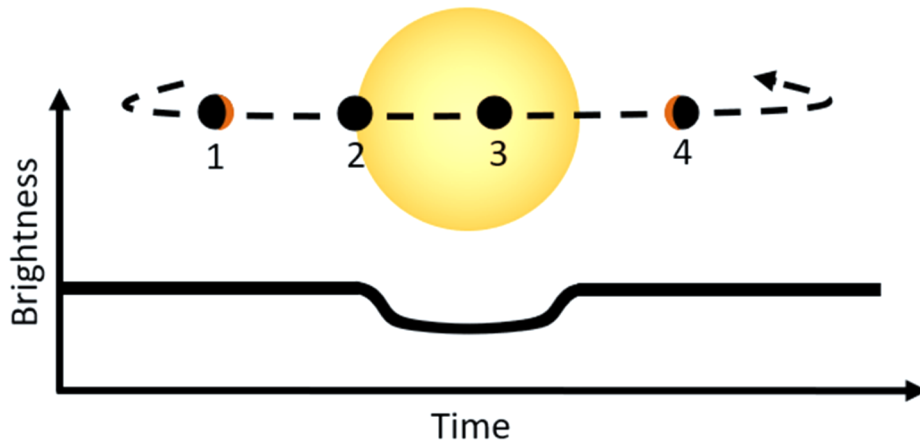


Figure 4: A depiction of an exoplanet at various points in its orbit around its host star. The light curve is a plot of the star's brightness over time, which is dependent on the exoplanet's position in its orbit [own work].

2.1.2 Radial Velocity Method

The radial velocity method of detecting exoplanets consists of observing the target star's spectrum over time. Any planets or other stars in a solar system will orbit the center of mass of the solar system and the star's spectrum will shift depending on the speed of its motion around the center of mass. As the star moves away from Earth, the wavelength will appear red-shifted as the wavelength appears longer than the true value. When the star is moving towards Earth, the wavelength will appear shorter as the light is blue-shifted. The magnitude of the red- or blue-shifting can be used to calculate the star's radial velocity and then the mass of planets in the system. This method is simplest with a two body system, but there exists observational techniques that are used when there is

more than one planet orbiting a star. Figure 5 depicts how the star's motion influences the wavelength of light as it is seen on Earth.

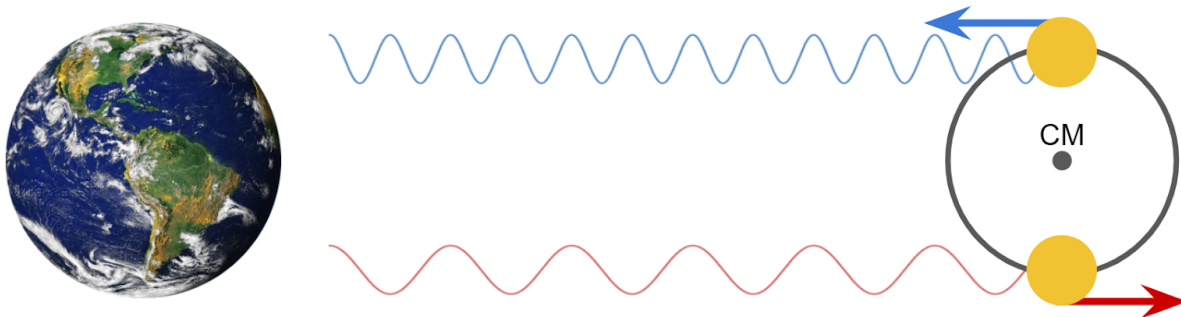


Figure 5: A diagram illustrating how a star's motion relative to earth can shift the wavelength of light from the star that we observe. Moving closer shortens the wavelength - blue shifting. Moving away stretches the wavelength - red shifting [own work].

2.2 Imaging Transits

2.2.1 Equipment and Software

The camera used to image the transits was an SBIG STXL-6303e CCD camera. A charge-coupled device (CCD) camera converts photons into an electrical current proportional to the amount of light incident on the camera's sensor via the photoelectric effect where a photon is absorbed and an electron is emitted. The CCD sensor utilizes a 2-dimensional array of coupled capacitors in an integrated circuit that allows charge to pass between the capacitors. Charge is stored in the sensor's capacitors throughout the camera's exposure time. After the exposure is complete, the charge is transferred through each capacitor into a series of individual voltages that are used to produce the image [5]. Regardless of any photon stimulation, there is an inherent dark current that flows through the CCD sensor's capacitors. Thermal noise is generated during longer sensor exposures. It's important to keep the CCD at a cool temperature to minimize this thermal noise. The CCD camera used to collect the data presented in this paper was kept at -30°C

during operation and has a dark current of $0.5 \text{ e}^-/\text{p/s}$. The pixel array is 3072×2048 pixels and each pixel is $9 \text{ }\mu\text{m} \times 9 \text{ }\mu\text{m}$ [2].

The UNH Observatory's Celestron C14 telescope was used to collect data. The C14 is a 14-inch Schmidt-Cassegrain telescope that combines mirrors and a Schmidt corrector plate used to improve the focus of the telescope. Spherical aberrations occur in imperfect spherical lenses and mirrors and the Schmidt corrector plate is an aspherical lens engineered to produce equal and opposite spherical aberrations to correct the focus of incident light rays. Figure 6 demonstrates how light should focus in a theoretically perfect lens and how it actually focuses in a real spherical lens. Figure 7 depicts how the Schmidt corrector plate is used to adjust the paths of light rays so they pass through the focal point of the reflector.

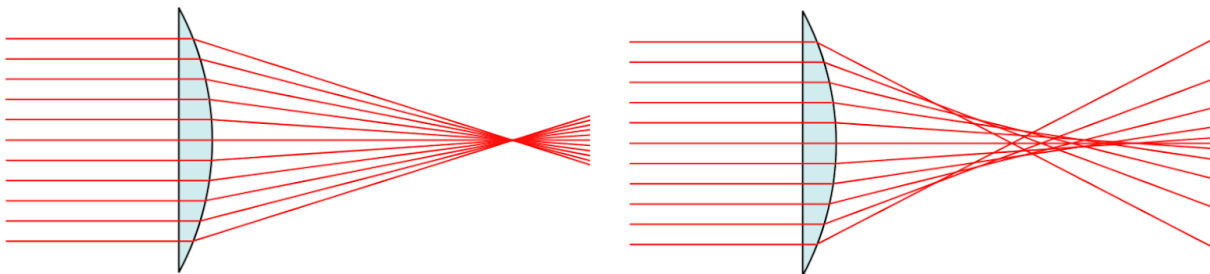


Figure 6: The left image depicts a perfect spherical lens where all light rays converge at the focal point. The right image shows a real spherical lens where the light rays do not converge due to imperfections in the lens ([Wikipedia](#)).

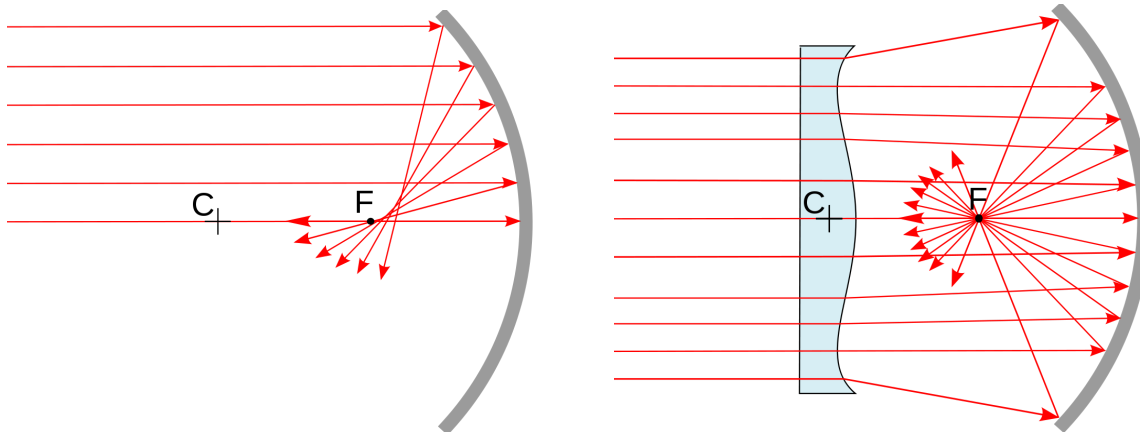


Figure 7: The left image shows the Cassegrain curved reflector plate without the Schmidt corrector plate and the rays do not converge on the focal point due to spherical aberrations in the reflector. The point marked C is the center of curvature and F is the focal point. The right image depicts how the corrector plate adjusts the ray paths so they converge on the focal point ([Wikipedia](#), Schmidt Corrector Plate by Jean-Jacques Milan).

The software used to guide the telescope is the Sky X Professional. This software contains a catalog of stars that it can direct the telescope to point to. The Sky X Professional software is useful for imaging transits because it can control both the telescope and the CCD camera.

The software used to analyze the transit images is AstroImageJ (AIJ) which is an image analysis software used to perform photometry [1]. Photometry is the process of converting an object's light into numerical values based on the intensity of that light. AIJ is able to perform photometry on a set of transit images by using other stars in the field of view as reference stars to determine when the target star's brightness is decreasing. Reference stars must be chosen carefully as they must not be variable stars, stars whose luminosity varies over small enough timescales to affect the photometry. AIJ is a powerful software tool that is able to account for factors such as orbital eccentricity, period, target star spectral class, etc, in the photometry calculations. The software also has a built-in

calibration function that takes in sets of calibration images to remove noise from the transit images. AIJ is the same software used by NASA's Transiting Exoplanet Survey Satellite (TESS) to analyze transit data.

2.2.2 Calibration Images

There are three types of calibration images used for the data in this paper. The first is dark frames, which are images taken with the shutter closed and for the same exposure time and ambient temperature as the science images. Dark frames are used to help account for the dark current that accumulates during the exposure. Their main function is to remove thermal noise that is generated throughout the exposure. Bias images essentially do not have an exposure time as they are taken at the fastest shutter speed the camera can handle. They are meant to calibrate the inherent readout noise of the sensor and camera. Bias images also help with dark current. Bias and dark images must both be taken at the same operating temperature as the transit images. Flat field images help to account for any dust or blemishes on the optics as well as vignetting. Vignetting occurs when there is less light around the edges of the images. Flat fields are taken by exposing the camera to a light source for an exposure time just long enough for the blemishes to appear; they do not have to be the same exposure as the transit images [8]. Figure 8 shows the three types of calibration images.

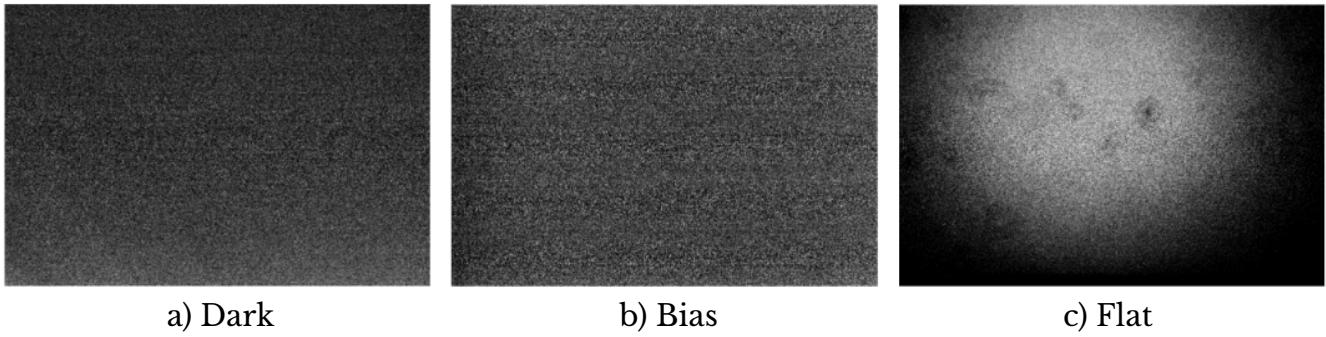


Figure 8: An example of each of the types of calibration images.

2.2.3 Method

Proper observing conditions are necessary in order to record a transit. The observing region of the sky must be clear of clouds. Ideally the entire sky would be free of clouds as they can move throughout the night with the wind and possibly drift over the target star. Clouds can also appear spontaneously during the transit, especially thin clouds at high altitudes. Cool air causes less distortions or “twinkling” of the incoming starlight. Dry air will minimize any moisture buildup on the telescope optics. The most important condition is that the observing location must be dark as too much sunlight or light pollution can impact the quality of the images. Bright moonlight can also decrease the quality of the images if the target star is in the same region of sky as the moon. The local observing conditions that cause light pollution will affect AIJ’s ability to accurately determine the brightness of the star throughout the transit.

There are many stars that are too dim to see with the unaided eye and telescopes help to gather more light with their large apertures. However, even with large apertures, some stars are still too dim. Cameras are useful because they can take long exposures to detect even the dimmest stars. TrES-1b is an 11.79 magnitude star [4] so a long exposure time on the camera was needed. The ideal exposure time for TrES-1b was 17 seconds.

To produce the best possible light curve, it is necessary to take images of the transiting system before and after the expected transit for ideally 30-60 minutes. This allows for a baseline measurement of the star's brightness out of transit so that AIJ can determine how much of a decrease in brightness occurred due to the planet. Following the post-egress baseline, a series of 10 dark, bias, and flat field images were captured to be used in calibration.

3 DATA ANALYSIS

TrES-1b transits every 3.03 days which results in the transit occurring about 43 minutes later every three days. As the transits occur later and later, they will begin to happen during the day and therefore cannot be observed. There was a period of time from Feb 24th, 2022 to Mar 8th, 2022 with 5 visible transits of TrES-1b. Of these, only Feb 27th and Mar 5th were observable transits due to local weather conditions during the other three transits.

3.1 Feb 27 Transit

Figure 9 depicts the light curve for the Feb 27 transit. At the beginning of the transit, the data is rather dispersed due to the transit beginning with the target star at only 17° in altitude. This caused the star's light to travel through a thick layer of atmosphere. There is less dispersion at the end of the data set due to the star having risen to 42° at the egress. Additionally, the observatory is generally unable to observe targets below ~10°, so the pre-ingress baseline was not as long as the ideal time of 30-60 minutes. This brightness plot does not take the normal shape of a light curve. A proper light curve levels out once the planet is fully in front of the host star, but the light curve for this transit does not level out until the middle of the transit. This is likely due to a thin, sporadic cloud cover

through the transit, causing the star to appear brighter than it was after the ingress. There was a thicker cloud cover that temporarily passed over the field of view close to the egress. The effects of these clouds can be seen around the egress where there is an increase in data dispersion. It is apparent that these clouds did not have a drastic effect on the data because the predicted egress corresponds to the flattening data points at the end of the transit.

Figure 10 shows a plot of two reference stars and their brightnesses during the transit. Their relatively flat distribution shows that they are not variable stars, so they are likely not responsible for the trends seen in figure 9. A simple method to confirm this assumption is to perform photometry on this data set again with different non-variable stars chosen. This was done with a second set of reference stars and the brightness plot was nearly identical to figure 9. The flat blue line seen at 1.00 on the vertical axis is a failed trend line because AIJ was unable to fit a proper light curve to the plot due to the data not following a typical light curve pattern. Due to the lack of a fit curve for the data, it is difficult to determine with certainty whether the apparent ingress and egress of the data truly match the predicted values or if it is merely a coincidence.

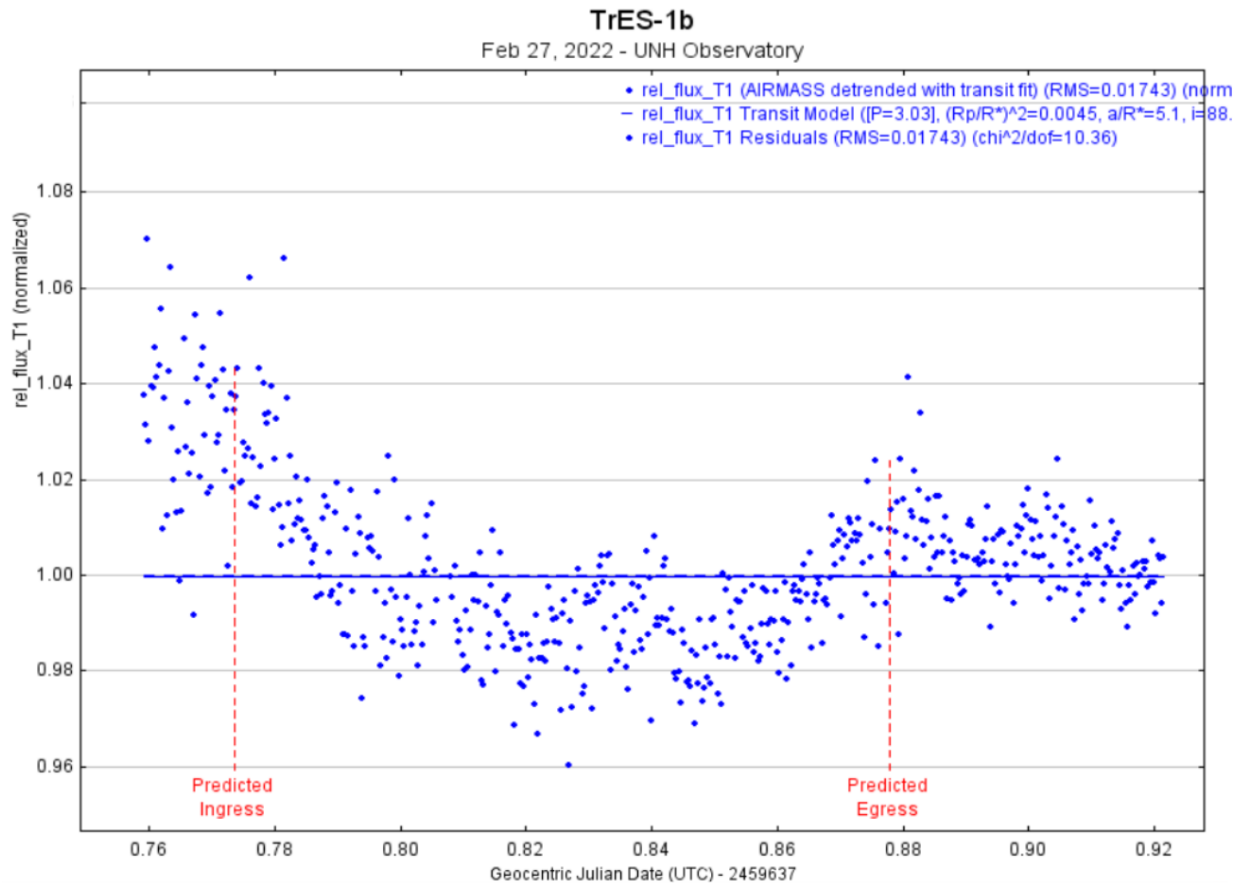


Figure 9: A light curve for the TrES-1b transit on Feb 27, 2022. The vertical axis represents the observed brightness of the star throughout the transit. The horizontal axis depicts the time of the transit in Julian days.

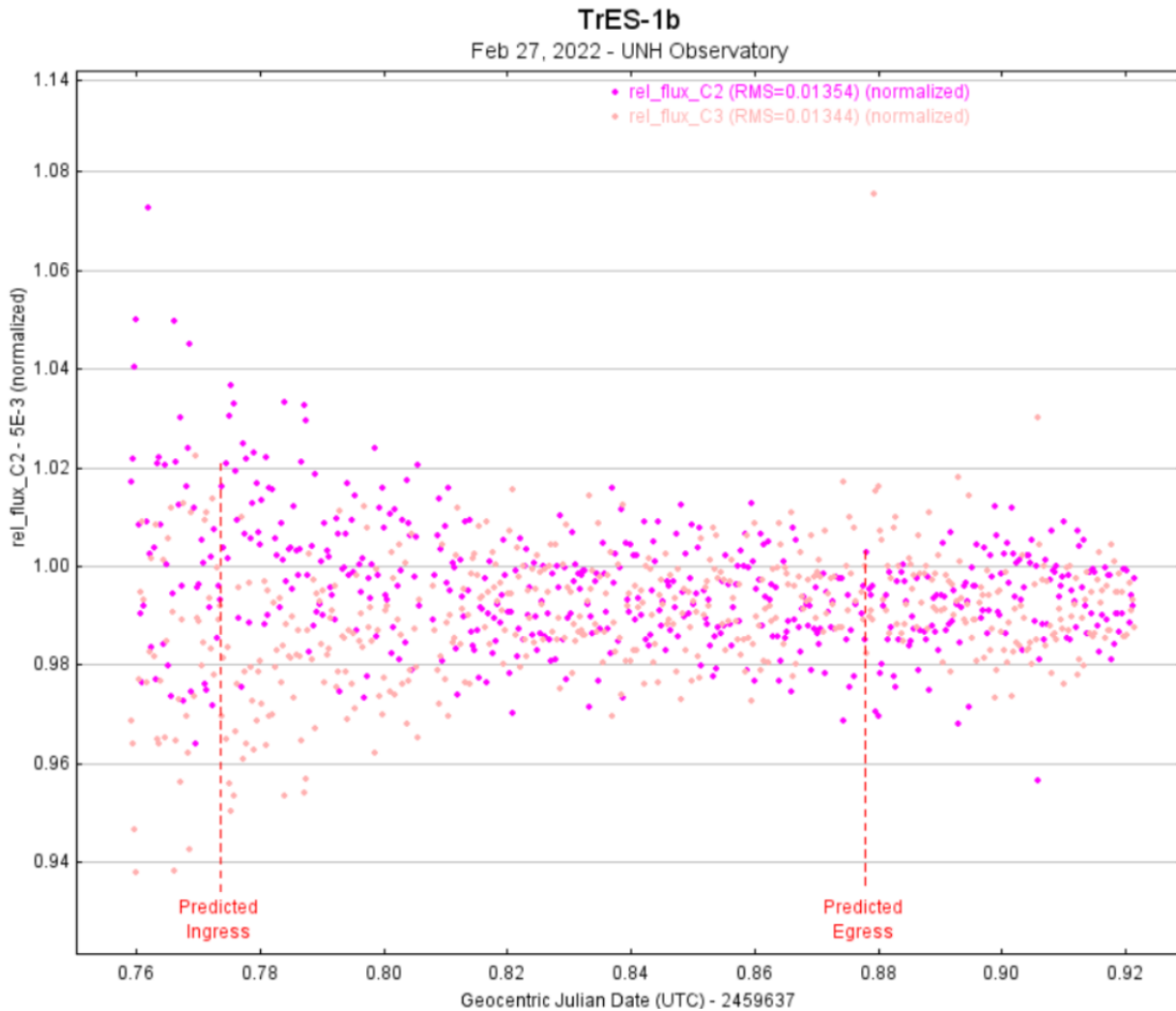


Figure 10: A light curve for the two reference stars used. The dispersion in the data before the ingress reinforces the error introduced by the star’s light having to pass through more of the atmosphere at low altitudes in the sky. The data points for the reference stars appear mirrored around a horizontal line in the center of the data set because AIJ takes the average of the brightness of the reference stars to determine the brightness of the target star.

3.2 Mar 5 Transit

The light curve for the Mar 5 transit can be seen in figure 11 and the brightness plot for the reference stars can be seen in figure 12. While there is an obvious period of decreased brightness, it is visible that this plot is inconsistent with what is to be expected for a light

curve. There are two main instances between the ingress and egress where the data flattens where it is not supposed to. The target star gained altitude throughout the transit and it began at 35° , so there is less general dispersion than the Feb 27 transit. The irregular pattern of the data around the egress can be attributed to the Sun rising and brightening the sky. The reference star plot in figure 12 shows a significant amount of variability in the stars' brightness, however the reference stars were confirmed to be non-variable. This trend is indicative that the data for this transit was adversely affected by the local sky conditions. AIJ was unable to fit a light curve to this data set as well due to the irregularities present in the transit images.

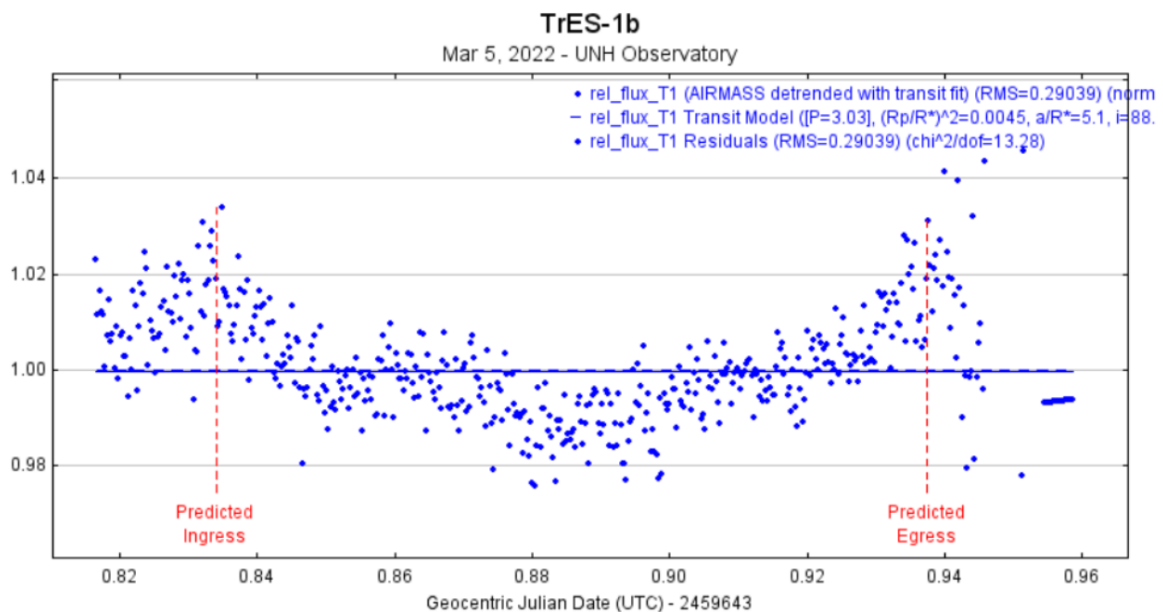


Figure 11: A light curve for the Mar 5 transit of TrES-1b.

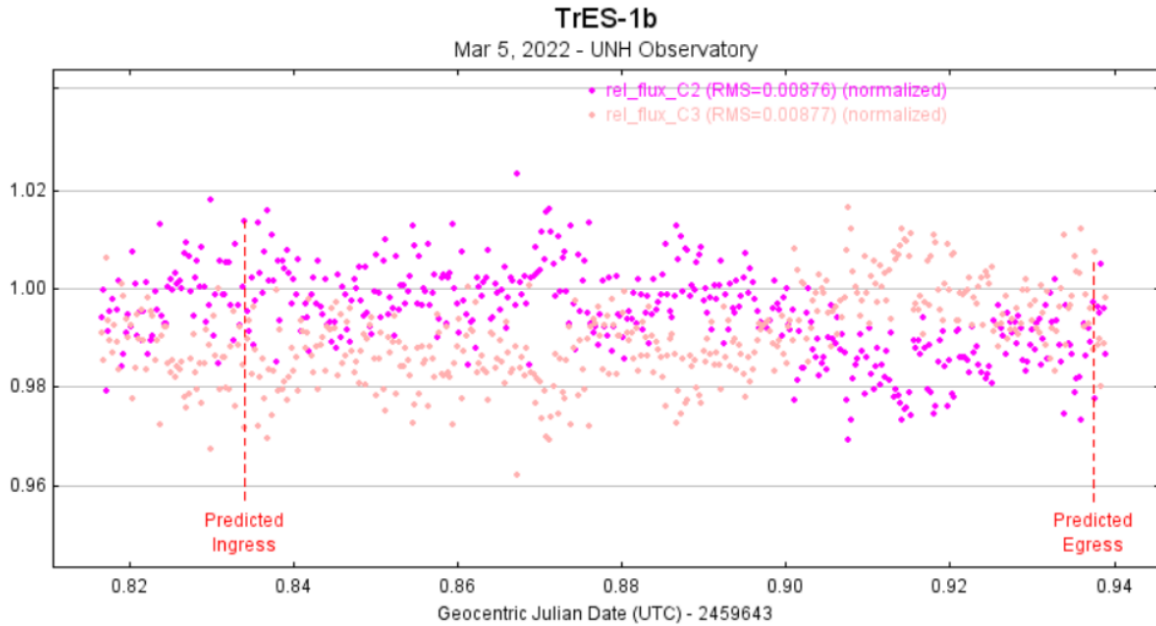


Figure 12: A brightness plot of the reference stars for the Mar 5 TrES-1b transit.

4 DISCUSSION

4.1 Conclusion

An accurate and reliable light curve is crucial to studying possible orbital decay in an exoplanetary system because they allow for the transit center, or mid-transit, to be determined. A transit center can be identified even from a partial transit where either the ingress or egress is missing, though having both will yield a more accurate value of the transit center. Transit center values for Feb 27 and Mar 5 were unable to be calculated.

The largest factor affecting AIJ's ability to fit a light curve to the brightness plots for each transit was the local weather and sky conditions. Cloud cover has a large effect on the data quality because it can nonuniformly reflect light into the telescope's aperture.

Nonoptimal telescope tracking was another source of error in the data sets. As the transit progressed, the telescope was unable to perfectly track the target star. This resulted in the star slowly moving across the CCD image through the transit. A depiction of this can be

seen in figure 13. This introduces error as the star moves to a different pixel on the sensor because the pixels aren't identical so they will all process the star's light differently.

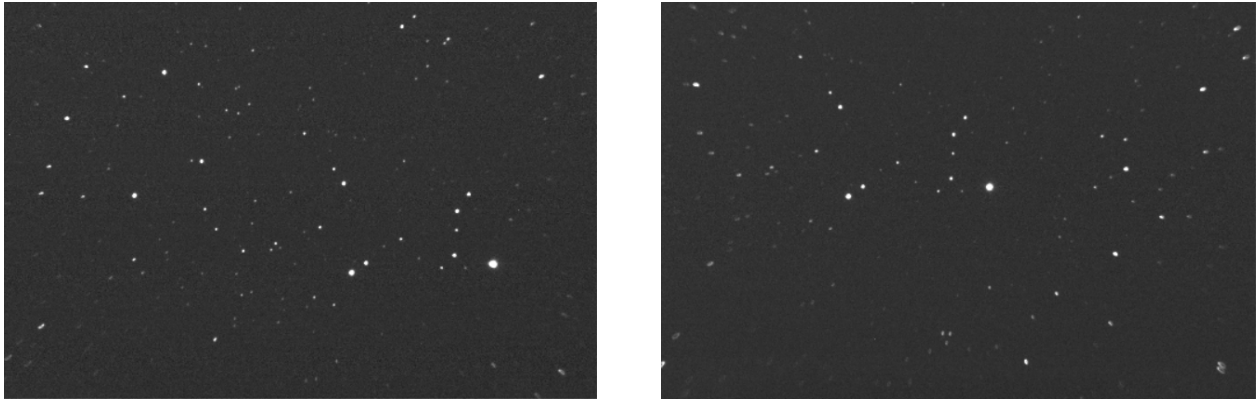


Figure 13: The left image shows the star field at the beginning of the transit. The right image shows how the star field shifted over ~2.5 hours after the left image was taken.

Sources of error in data taken by ground-based observatories are to be expected due to atmospheric interference and local weather, so data is best taken from space-based observatories. It's important to have reliable light curves and thus transit centers because they are used to create orbital decay plots like the ones seen in figures 1 and 2. The observed transit center is compared to the calculated (theoretical) transit center, which can be found in places like the Exoplanet Transit Database (ETD). These orbital decay plots can help to better understand what mechanisms are at play in exoplanetary systems to cause orbital decay. Studying other planetary systems in different phases of their evolution can aid in improving the current understanding of solar system formation, dynamics, and evolution over time.

4.2 Future Work

The TrES-1b system will be further analyzed using data that other astronomers have submitted to the ETD in the last several years. Additional transits of TrES-1b will be observed and combined with the ETD data to create orbital decay plots. Several fit lines including a fit for orbital decay, apsidal precession, and constant period will be applied to the decay plot and statistically analyzed with the Bayesian Information Criterion (BIC) to determine which model best describes the TrES-1 system. The methods discussed in this paper will be applied to the Wasp-10 system after a deeper analysis of TrES-1b is performed. A tracking method called auto-guiding will be applied to the telescope's mount and control system to improve the quality of the transit images to reduce the source of error associated with the star field drifting across the image during the transit.

Acknowledgements

I would like to thank J. Gianforte and S. Hagey for their continued support and guidance throughout my project. I would also like to thank J. Gianforte and C. Lopate for their assistance in evaluating this paper.

REFERENCES

- [1] AstroImageJ User Guide. URL: https://www.astro.louisville.edu/software/astroimagej/guide/AstroImageJ_User_Guide.pdf
- [2] Diffraction Limited. URL: <https://diffractionlimited.com/product/stxl-6303/>
- [3] The Extrasolar Planets Encyclopaedia. URL: <http://exoplanet.eu/>
- [4] The Exoplanet Transit Database. URL: <http://var2.astro.cz/ETD/predictions.php>
- [5] Amelio, G. F., "Charge-Coupled Devices". *Scientific American*. 230 (2).
- [6] Alonso, R., et al. TrES-1: The Transiting Planet of a Bright K0V Star. *The Astrophysical Journal Letters*. 613: 153–156. (2004). doi.org/10.1086/245256.
- [7] Ballesteros, F. J., Fernandez-Soto, A., Martinez, V.J., Diving into Exoplanets: Are Water Seas the Most Common?. (2019). <https://doi.org/10.1089/ast.2017.1720>
- [8] Gary, B., *Exoplanet Observing for Amateurs*. (pp. 42-44) (2007).
- [9] Nesvorný, D., et al., The Detection and Characterization of a Nontransiting Planet by Transit Timing Variations. *Science*, Volume 336, Issue 6085, (2012), Pages 1133-1136, <https://doi.org/10.1126/science.1221141>
- [10] Oort, D., A Search for Orbital Decay in Close-in Exoplanetary Systems. (2015). https://www.academia.edu/34375454/A_Search_for_Orbital_Decay_in_Close_in_Exoplanetary_Systems
- [11] Southworth, J., Homogeneous studies of transiting extrasolar planets – III. Additional planets and stellar models, *Monthly Notices of the Royal Astronomical Society*, Volume 408, Issue 3, (2010), Pages 1689–1713, <https://doi.org/10.1111/j.1365-2966.2010.17231.x>
- [12] Steffen, J. H., Agol, E., An analysis of the transit times of TrES-1b, *Monthly Notices of the Royal Astronomical Society: Letters*, Volume 364, Issue 1, (2005), Pages L96–L100, <https://doi.org/10.1111/j.1745-3933.2005.00113.x>
- [13] Wolszczan, A., Frail, D. A planetary system around the millisecond pulsar PSR1257 + 12. *Nature* 355, 145–147 (1992). <https://doi.org/10.1038/355145a0>